

The dust production rate of AGB stars in the Magellanic Clouds

Raffaella Schneider^{1*}, Rosa Valiante¹, Paolo Ventura¹, Flavia dell’Agli¹,
Marcella Di Criscienzo^{1,2}, Hiroyuki Hirashita³ and Francisca Kemper³

¹INAF/Osservatorio Astronomico di Roma, Via di Frascati 33, 00040 Monteporzio, Italy

²INAF/Osservatorio Astronomico di Capodimonte, Salita Moiarello 16, 80131 Napoli, Italy

³Institute of Astronomy and Astrophysics, Academia Sinica, PO Box 23-141, Taipei 10617, Taiwan

ABSTRACT

We compare theoretical dust yields for stars with mass $1 M_{\odot} \leq m_{\text{star}} \leq 8 M_{\odot}$, and metallicities $0.001 \leq Z \leq 0.008$ with observed dust production rates (DPR) by carbon-rich and oxygen-rich Asymptotic Giant Branch (C-AGB and O-AGB) stars in the Large and Small Magellanic Clouds (LMC, SMC). The measured DPR of C-AGB in the LMC are reproduced only if the mass loss from AGB stars is very efficient during the carbon-star stage. The same yields over-predict the observed DPR in the SMC, suggesting a stronger metallicity dependence of the mass-loss rates during the carbon-star stage. DPR of O-AGB stars suggest that rapid silicate dust enrichment occurs due to efficient hot-bottom-burning if $m_{\text{star}} \geq 3 M_{\odot}$ and $Z \geq 0.001$. When compared to the most recent observations, our models support a stellar origin for the existing dust mass, if no significant destruction in the ISM occurs, with a contribution from AGB stars of 70% in the LMC and 15% in the SMC.

Key words: Stars: AGB and post-AGB, supernovae: general. ISM: dust, extinction. Galaxies: Magellanic Clouds, evolution, ISM

1 INTRODUCTION

The best way to compare the total dust input from evolved stars in a galaxy to the total dust budget is to detect the entire population of dusty stars at infrared (IR) wavelengths and estimate the dust-injection rate of each. These global measurements are not possible in our Galaxy, due to source confusion in the Galactic plane, but have been attempted on nearby external galaxies, such as the Small and Large Magellanic Clouds (hereafter SMC and LMC, respectively). Extragalactic studies have also the advantage that distances to sources within a galaxy can be assumed to be the same.

The importance of the Magellanic Clouds as laboratories of dust enrichment by stellar sources has been thoroughly discussed in the literature (Matsuura et al. 2009, 2013; Srinivasan et al. 2009; Boyer et al. 2012; Riebel et al. 2012). A growing body of observational data has been made available to the community by means of dedicated large photometric surveys. Among the others, the Magellanic Clouds Photometric Survey (MCPS, Zaritsky et al. 2004), the Two Micron All Sky Survey (2MASS, Skrutskie et al. 2006), Surveying the Agents of a Galaxy’s Evolution Survey (SAGE)

with the *Spitzer* Space Telescope (SAGE-LMC, Meixner et al. 2006; SAGE-SMC, Gordon et al. 2011), and *HERschel* Inventory of The Agents of Galaxy Evolution (HERITAGE, Meixner et al. 2010, 2013) have provided catalogues of point sources as well as high-resolution maps of the emission by the warm and cold dust components in the interstellar medium (ISM).

In addition, a wealth of complementary data allows to reconstruct the recent and past star formation histories of the galaxies (see, among others, Harris & Zaritsky 2004, 2009; Bolatto et al. 2011; Skibba et al. 2012; Weisz et al. 2013; Cignoni et al. 2013), their metal enrichment histories (see e.g. Carrera et al. 2008a, 2008b; Piatti 2012; Piatti & Geisler 2013), and their present-day global gas, stellar and dust content (see Meixner et al. 2013 for a recent collection of observational data).

Hence, these two galaxies represent an excellent astrophysical laboratory to investigate the life-cycle of dust in the ISM, providing a fundamental benchmark to theoretical models.

Knowledge of the amount and composition of dust formed by stars of intermediate mass ($1 M_{\odot} \leq m_{\text{star}} \leq 8 M_{\odot}$) and in the ejecta of core-collapse supernovae ($m_{\text{star}} > 8 M_{\odot}$, where m_{star} is the stellar mass at zero-age main sequence)

* E-mail: raffaella.schneider@oa-roma.inaf.it

represents the first step towards the understanding of dust enrichment from the most distant galaxies to the Local Universe. The relative importance of these stellar sources of dust depends on the mass-dependent dust yields, on the stellar initial mass function (IMF), as well as on the star formation history (SFH) of each galaxy (Valiante et al. 2009, 2011). Contrary to previous claims, dust production at high redshifts, $z > 6$, is not necessarily driven by massive stars, as stars of intermediate mass on their Asymptotic Giant Branch (AGB) can dominate dust production on a timescale which ranges between 150 and 500 Myr (Valiante et al. 2009). Local observations of dust emission in the circumstellar shells of evolved stars or in recent supernovae and supernova remnants have the potential to significantly reduce uncertainties associated to theoretical dust yields.

In this paper, our main aim is to compare dust production rates by AGB stars calculated by means of theoretical models to observations of evolved stars in the Magellanic Clouds. In particular, we consider a new grid of dust yields for different stellar masses and metallicities (Ventura et al. 2012a, 2012b, Di Criscienzo et al. 2013; Ventura et al. 2014) which is based on models calculated with a full integration of the stellar structure, following the evolution from the pre-main sequence phase using the code ATON (Ventura et al. 1998; Ventura & D’Antona 2009). This represents an important difference with respect to previous studies by Ferrarotti & Gail, whose dust yields are based on stellar properties computed from synthetic¹ models (Ferrarotti & Gail 2001, 2002, 2006; Zhukovska, Gail & Tieloff 2008) or with respect to more recent hybrid models where the integration is limited to the envelope structure of the stars (Marigo et al. 2013; Nanni et al. 2013). As a consequence, the mass and metallicity dependence of carbon and silicate dust yields based on ATON stellar models can not be reproduced by dust yields based on synthetic models, due to the different treatment of physical processes, such as the third dredge-up and the hot bottom burning, which alter the surface chemistry of AGB stars (Ventura et al. 2014).

By comparing the predictions of different sets of AGB stars dust yields to observations of carbon-rich and oxygen-rich AGB stars in the Magellanic Clouds, we can hope to constrain some of the model uncertainties. In addition, the difference in the gas metallicity of the two galaxies, with $Z_{\text{SMC}} = 0.004$ and $Z_{\text{LMC}} = 0.008$, allows to explore the complex and poorly understood dependence of AGB stars dust production rates on their progenitors initial metallicity (Ventura et al. 2012b). Finally, we can assess the relative importance of AGB stars and supernovae as dust producers in the two galaxies, comparing the overall contribution of stellar sources to the estimated total dust mass in the ISM.

In a recent paper, Zhukovska & Henning (2013) have done a similar analysis, discussing the dust input from AGB stars in the LMC. For the first time, theoretically calculated dust production rates of AGB stars have been compared to those derived from IR observations of AGB stars for the entire galaxy. In their comparison, they consider synthetic yields by Zhukovska et al. (2008) but discuss also the im-

plications of their models when ATON yields are adopted. They find that while synthetic models lead to carbon and silicate dust production rates in good agreement with observations, ATON (hereafter **old** ATON) models under-predict carbon-dust production rates, favouring silicate dust production, in contrast to the observations. Motivated by these findings, we have recently investigated the dependence of the predicted dust yields on the macrophysics adopted to describe the AGB evolution (Ventura et al. 2014) and a new grid of ATON (hereafter **new** ATON) dust yields has been computed for different initial metallicities, which range between 3×10^{-4} to 8×10^{-3} , including the metallicity of the SMC, $Z = 0.004$, that has not been considered in previous calculations.

Here we extend the comparison to this new ATON grid. In addition, we do not limit the analysis to AGB stars in the LMC but we test the models against observations in the SMC.

The paper is organized as follows: in Section 2, we briefly summarize the AGB stellar dust yields predicted by different theoretical models; in Section 3 we review the observationally constrained star formation and chemical enrichment histories of the Magellanic Clouds; the associated dust production rates for different sets of dust yields are presented in Section 4 and compared to observational data. The best fit models are then used, in Section 5, to assess the role of AGB stars and supernovae in the global dust budget of the LMC and SMC. Finally, in Section 6 we summarize and discuss our conclusions.

2 DUST YIELDS FROM AGB STARS

Theoretical calculations of the total dust mass formed during the AGB phase has recently attracted many independent studies. In their pioneering work, Ferrarotti & Gail (2001, 2002, 2006) used synthetic stellar evolution models to compute the non-equilibrium grain condensation and estimated the dust yields for M, S, and C-type AGB stars of different ages and metallicities (Zhukovska, Gail & Tieloff 2008). These models have proved to be very useful tools, thanks to the simplicity with which they can be incorporated into stellar population synthesis studies and chemical evolution models (Zhukovska & Henning 2013). However, their major drawback is to rely on simple evolutionary codes where some physical processes, such as the variation of the core mass, the temperature at the bottom of the convective envelope, the core mass at which the Third Dredge Up (TDU) begins to operate, the extent of the inwards penetration of the surface convective zone, are described by means of analytic approximations (Marigo & Girardi 2007). Since these processes affect the chemical composition and physical conditions in the circumstellar atmosphere during the AGB phase, they also affect the resulting dust mass and composition.

To overcome this limitation, in a series of papers we have recently published a grid of AGB stars dust yields for different stellar masses and metallicities using models that follow stellar evolution from the pre-main sequence phase until the almost complete ejection of the stellar mantle by means of the code ATON (Ventura et al. 1998; Ventura & D’Antona 2009). In the first paper of the series, Ventura et al. (2012a) computed the mass and composition of dust pro-

¹ In this context, by synthetic models we refer to models in which the evolution is described with analytical relations derived by fitting the results of full evolutionary models.

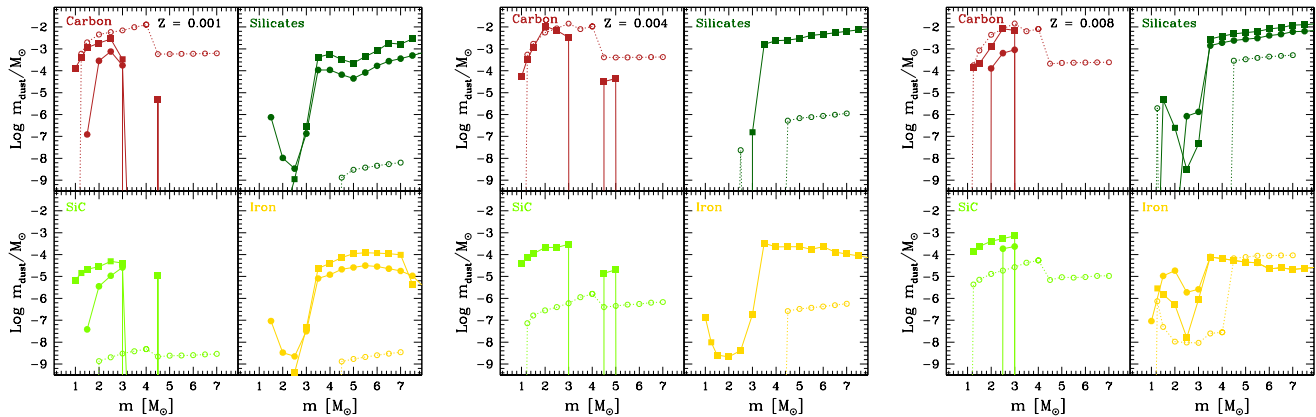


Figure 1. Dust yields from AGB stars as a function of their initial mass for three initial metallicities: $Z = 0.001$, 0.004 , and 0.008 (left, central, and right panels, respectively), with separate contributions from carbon dust, silicates, SiC and Iron grains. In each panel, empty squares show the predictions from Zhukovska et al. (2008), filled circles and squares are the old and new ATON yields, respectively (see text).

duced by stars with masses in the range $1M_{\odot} \leq m \leq 8M_{\odot}$ and with a metallicity of $Z = 0.001$ during their AGB and super-AGB phases. They found that the dust composition depends on the stellar mass: low-mass stars, with $m < 3M_{\odot}$, produce carbon dust whereas more massive stars experience Hot Bottom Burning, do not reach the C-star stage and produce silicates and iron grains.

Starting from a higher initial metallicity, $Z = 0.008$, Ventura et al. (2012b) found a similar trend, with a transition between carbon and silicate dust production occurring at a threshold mass of $3.5M_{\odot}$. While the yields of carbon dust do not depend on metallicity, the mass of silicate dust grows with metallicity due to the combined effect of the softer HBB experienced and of the larger silicon abundance.

Conversely, for stars with initial metallicity $Z < 0.001$, no silicate dust formation occurs due to the scarcity of silicon available in the envelope; carbon dust continue to form in stars with masses $\leq 2.5M_{\odot}$ down to initial metallicities of $Z = 3 \times 10^{-4}$, below which even these low-mass stars experience HBB, do not become carbon stars and AGB stars do not produce any dust (Di Criscienzo et al. 2013).

It is important to stress that some of these results could not be captured by previous models as they heavily depend on fundamental physical processes occurring during the AGB evolution. In particular, the TDU and the Hot Bottom Burning (HBB) alter the surface chemistry of AGB stars. Silicate dust production depends on the modelling of convection which, in turns, determines the strength of HBB. On the other hand, the mass of carbon dust formed depends on the extent of the third dredge-up: a small amount of extra-mixing from the borders of the convective shell developed during the thermal pulses favour a much larger penetration of the convective envelope, leading to a much stronger third dredge up, hence a larger carbon dust production. These issues have been thoroughly discussed by Ventura et al. (2014), who explored the impact of different physical assumptions concerning the extra-mixing and mass-loss during the C-star phase on the resulting dust yields. In Fig. 1, we show the AGB stars dust yields predicted by the old and new ATON models. For comparison, we also show

the dust yields predicted by Zhukovska et al. (2008) using synthetic AGB stellar models (hereafter Z08 AGB stars dust yields). A detailed analysis of the differences between the different grids of dust yields has been given in Ventura et al. (2014) and we refer the interested reader to the original paper for more details. Here we limit the discussion to the features which are of interest for the purpose of our study, namely the mass and metallicity dependence of carbon dust and silicates. In particular, it is evident from Fig. 1 that the new ATON models predict larger carbon (and SiC) dust yields with respect to the old ATON models, independent of the initial stellar metallicity. This is due to the effect of the extra-mixing (larger efficiency of TDU) and - to a larger extent - to the increased mass loss rates in the C-star stage. In the new ATON models mass loss during the C-star stage is described following the formulation by Wachter et al. (2008) which accounts for carbon-dust production and the consequent acceleration of the wind. For all the other evolutionary phases, the mass loss prescription by Bloeker (1995) is used, similarly to the old ATON models. The mass of silicates (and iron) dust produced by AGB stars with larger mass is larger in the new ATON models, particularly for the lowest metallicity, due to the stronger HBB experienced.

The largest difference between ATON and Z08 dust yields concerns the behaviour of AGB stars with initial masses $> 3M_{\odot}$: these contribute to carbon-dust production according to Z08, but never reach the carbon-star stage according to ATON models. This difference is due to the different treatment of convection, that reflects into a much stronger HBB experienced by our models, in comparison to Z08, causing the difference in the predicted silicate dust production. It is important to note that the mass segregation between carbon dust production by low-mass AGB stars and silicate dust production by high-mass AGB stars is a feature unique to our dust models, and it is not apparent in the models by Zhukovska et al. (2008) nor in the most recent models by Nanni et al. (2013). We do not show in the figure the results of the latter study as these are qualitatively in good agreement with those of Zhukovska et al. (2008). In fact, although Nanni et al. (2013) have based their calculation

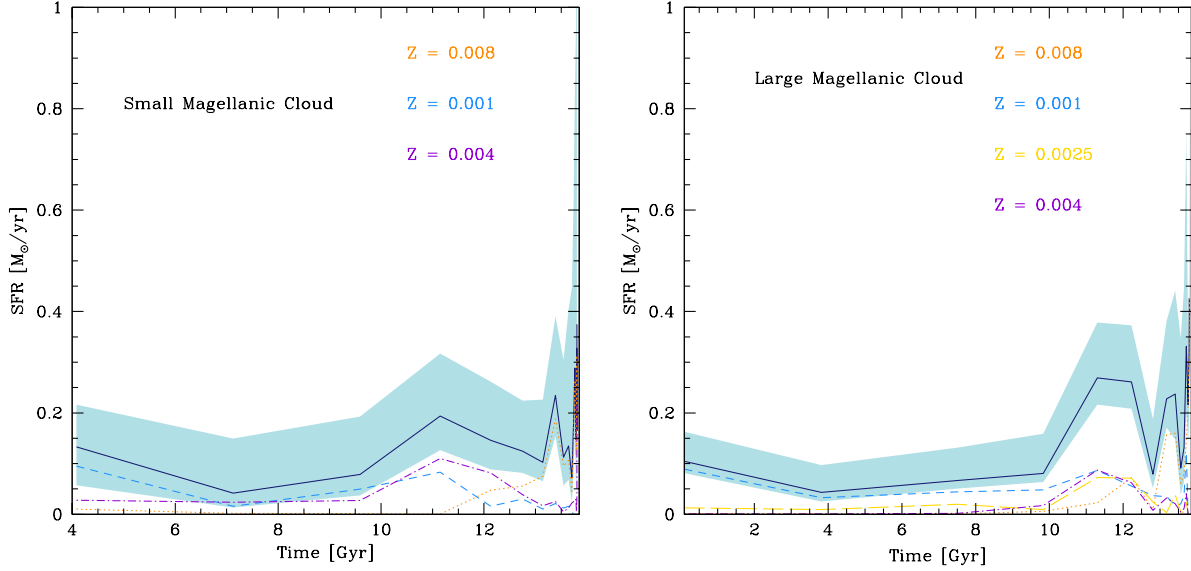


Figure 2. The star formation history of the Small (left panel) and Large (right panel) Magellanic Clouds as a function of time from Harris & Zaritsky (2004, 2009). The solid lines show the best-fit star formation history, with shaded regions representing the uncertainty on the fit. The separate contribution of different metallicity bins is also shown with $Z = 0.001, 0.0025, 0.004$, and 0.008 plotted as dashed, long-dashed, dot-dashed, and dotted lines, respectively. The star formation history for the SMC starts at 4 Gyr as the oldest stellar age bin in Harris & Zaritsky (2004) is 9.988 Gyr.

on a complete envelope model that represents a significant step forward with respect to purely synthetic AGB models, their approach does not follow the complete stellar evolution. It is important to stress that the HBB phenomenon, which is responsible for the large differences in the mass and composition of dust produced by high-mass AGB stars, is a consequence of the delicate coupling between the outer region of the degenerate core, the CNO burning layer, and the innermost regions of the surface convective zone; *by definition, this cannot be described within the framework of a synthetic modelling of the AGB phase.*

3 THE STAR FORMATION AND METAL ENRICHMENT HISTORIES OF THE MAGELLANIC CLOUDS

Spatially resolved star formation histories of the SMC and LMC have been obtained by Harris & Zaritsky (2004, 2009) based on the Magellanic Clouds Photometric Survey (MCPS), which includes over 6 million SMC stars and 20 million LMC stars. The star formation history of each observed stellar population is obtained minimizing the difference between observed and synthetic color-magnitude diagrams (CMD) selected from a library generated by means of the StarFISH code (Harris & Zaritsky 2001) spanning appropriate ranges in metallicity and ages. Adopting a Salpeter Initial Mass Function (IMF), with a binary fraction of 0.5, the star formation rate as a function of the stellar ages for 3 (4) metallicity bins has been inferred for 350 (1376) regions of the SMC (LMC). In Fig. 2 we show the total best-fit star formation history (solid lines, with the shaded region representing the uncertainty on the fit) and the separate contribution of different metallicity bins.

There are several temporally coincident features in the global star formation histories of the two galaxies, suggesting a common evolution for the Magellanic Clouds. Both galaxies experienced a long ($\sim 5 - 7$ Gyr) quiescent epoch starting roughly 10 Gyr ago, followed by a peak in the star formation rate roughly 2-3 Gyr ago and an enhanced star formation activity around 400 Myr ago (Harris & Zaritsky 2004, 2009). The best-fit global present-day star formation rates are $0.39 M_{\odot}/\text{yr}$ and $0.37 M_{\odot}/\text{yr}$, for the LMC and SMC, respectively. Note that the smallest age bin used in the photometric analysis is $\log(t_{\text{age}}/\text{yr}) = 6.8$ (6.6) for the LMC (SMC) and that the uncertainties on the fit at smaller stellar ages are quite large, with values in the range $[0.25 - 0.82] M_{\odot}/\text{yr}$ ($[0.13 - 5.7] M_{\odot}/\text{yr}$) for the LMC (SMC).

Wide-field ground-based surveys, as MCPS, provide spatially comprehensive coverage, but the resulting CMDs only extend below the oldest main-sequence turnoff. As a result, the ancient ($> 4 - 5$ Gyr) SFH can not be well constrained. To overcome this limitation, SFH studies have been done using the *Hubble Space Telescope* (HST), targeting - however - only a limited number of fields (see e.g. Cignoni et al. 2012, 2013; Weisz et al. 2013). Comparison between different studies is made difficult by the use of different assumptions regarding the stellar IMF, mass range, binary fraction and by the different spatial coverage of the galaxies. In Cignoni et al. (2012), the authors have derived the SFH for the two most crowded regions of the SMC; in their Fig. 22, they show that the SFHs by Harris & Zaritsky (2004) for the same regions show a significantly higher stellar production prior to 8.4 Gyr ago. A comparison between the normalized cumulative star formation histories is shown in the left panel of Fig. 3; the solid lines with shaded region represent the predictions of Harris & Zaritsky and the dashed lines are the recent results of Weisz et al. (2013)

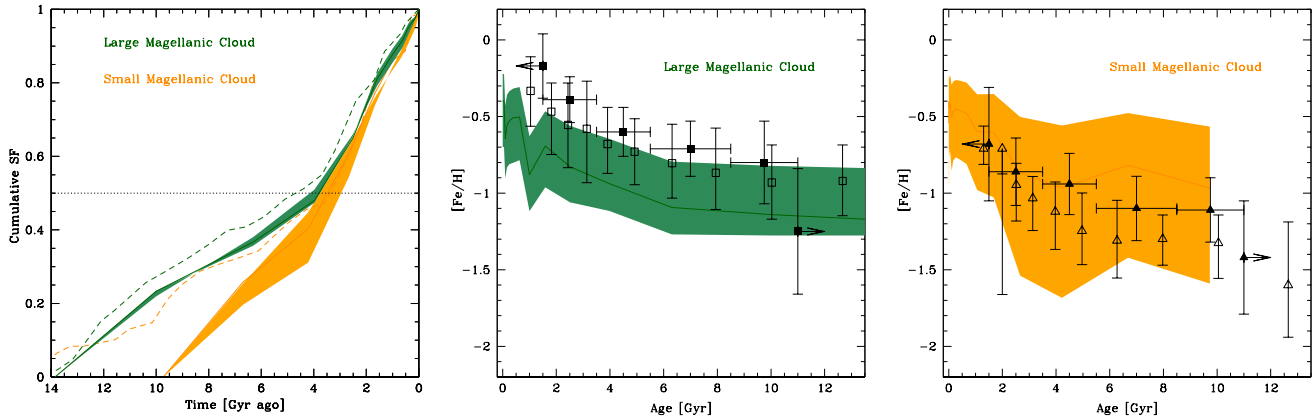


Figure 3. The left panel shows the cumulative star formation histories of the Magellanic Clouds corresponding to the results shown in Fig. 2. The dashed lines illustrate the recent results of Weisz et al. (2013) using deep HST data (see text). For illustrative purposes, the horizontal dashed line indicates 50% of the total stellar mass. The central and right panels show the age-metallicity relation obtained from the best-fit solution of Harris & Zaritsky (2004, 2009) for the Magellanic Clouds. Filled squares (triangles) are the average results obtained by Carrera et al (2000a) for the LMC disk population (SMC); the average results obtained by Piatti & Geisler (2013) for the LMC and by Piatti (2012) for the SMC are shown with empty squares and triangles, respectively.

who used HST archival data. The LMC (SMC) formed 50 per cent of its mass $\sim 4 - 6$ Gyr ($\sim 3 - 4$ Gyr) ago and both galaxies show a dramatic rise in SFR $\sim 3.5 - 4$ Gyr ago. Similar features are found in HST-based studies, although deeper data seem to suggested a larger cumulative star formation history at earlier epochs.

Using H_α and $24\mu\text{m}$ emission to trace recent unobscured and obscured star formation, Bolatto et al. (2011) have predicted a present-day global star formation rate of $0.037 M_\odot/\text{yr}$ for the SMC. Following a similar approach, Skibba et al. (2012) have estimated present-day star formation rates in the range $[0.016 - 0.039] M_\odot/\text{yr}$ for the SMC and $[0.25 - 0.63] M_\odot/\text{yr}$ for the LMC. While the latter values are in good agreement with the prediction by Harris & Zaritsky (2009), the former values seem to suggest a present-day star formation rate which is a factor of ten smaller than the results found by Harris & Zaritsky (2004); even accounting for the large uncertainties associated to the best fit value, different SMC observations do not appear to be consistent.

It is not surprising, therefore, that while the integrated star formation history of the LMC leads to a present-day stellar masses of $M_{\text{star}} = 1.1 \times 10^9 M_\odot$, in good agreement with the value inferred from IR observations by Skibba et al. (2012), the integrated stellar mass predicted by Harris & Zaritsky (2004) for the SMC is $1.21 \times 10^9 M_\odot$, almost a factor of 4 larger than the value inferred from IR data (see the left panels of Figs. 7 and 8 in section 5).

Hence, there are independent lines of evidence which seem to suggest that the recent star formation rate predicted by Harris & Zaritsky (2004) for the SMC may be over-estimated or that H_α and IR observations may have missed a significant fraction of obscured star formation (although this seems unlikely, given that the dust-to-gas ratio in the SMC is $1/1000$, approximately a factor of 5 smaller than the Milky Way, Leroy et al. 2007).

In what follows, we will use the star formation histories for the LMC and SMC predicted by Harris & Zaritsky (2004, 2009), with the caveat that while the former appears to be

robust, the latter should be taken with caution, as different studies do not appear to converge on the same result.

In the center and right panels of Fig. 3 we compare the age metallicity relation implied by the metallicity-dependent star formation histories of Harris & Zaritsky (2004, 2009) with the average data inferred by Carrera et al. (2008a, 2008b) using metallicities measured from spectroscopic data on individual stars (filled symbols) and with the results of Piatti (2012) and Piatti & Geisler (2013) who used deep photometric data on a large database of field stars (empty symbols). While the chemical evolution obtained by Harris & Zaritsky (2004, 2009) is in good agreement with metallicity and age measurements for star clusters, the best-fit age-metallicity relation of the LMC appears to be lower than the observational data for field stars. The agreement improves if the uncertainties due to the limited numbers of metallicity bins is considered. For this reason, in what follows we will show the model predictions adopting the best fit star formation (and chemical evolution) histories and the corresponding lower and upper limits.

4 DUST PRODUCTION RATE

Estimating the total dust production rate contributed by evolved stars requires the identification of point sources in a survey of a galaxy at near- and mid-infrared wavelengths, which are especially suitable to study thermal dust emission. The Magellanic Clouds have been mapped by large photometric surveys, such as the Magellanic Clouds Photometric Survey (MCPS, Zaritsky et al. 2004), the Two Micron All Sky Survey (2MASS, Skrutskie et al. 2006), Surveying the Agents of a Galaxy's Evolution Survey (SAGE) with the *Spitzer* Space Telescope (SAGE-LMC, Meixner et al. 2006; SAGE-SMC, Gordon et al. 2011), and *HERschel* Inventory of The Agents of Galaxy Evolution (HERITAGE, Meixner et al. 2010, 2013). Spectroscopic follow-up to the SAGE surveys has provided fundamental information for the spectral clas-

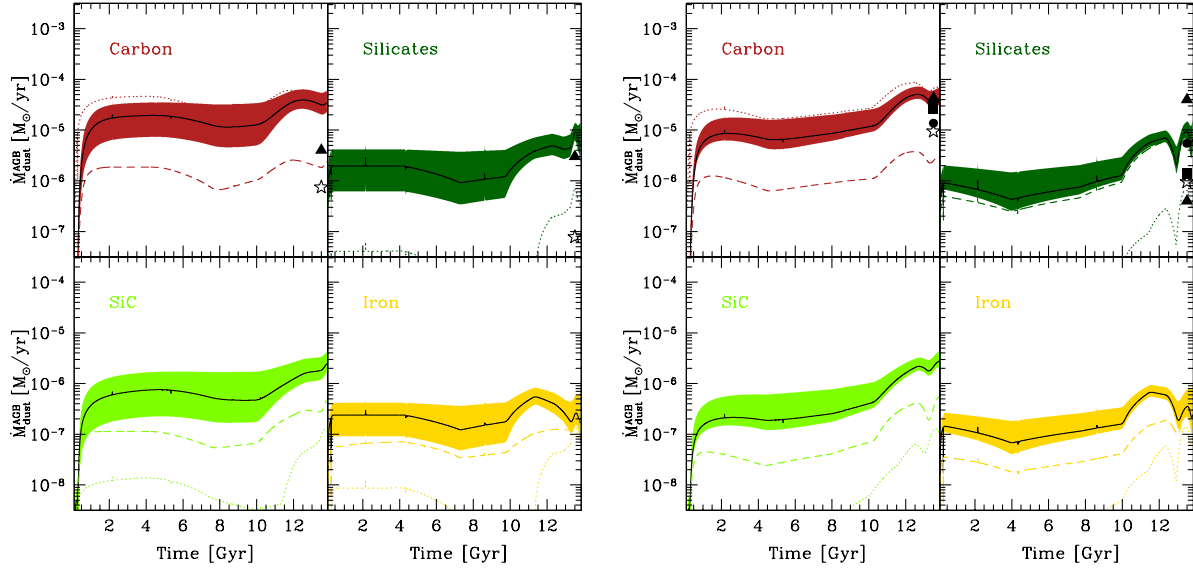


Figure 4. The dust production rate (DPR) of AGB stars in the Small (left panel) and Large (right panel) Magellanic Clouds as a function of time using the Harris & Zaritsky (2004, 2009) metallicity-dependent star formation histories. The solid lines show the predicted DPRs using the new ATON AGB yields, with shaded regions representing the uncertainty on the best-fit star formation histories. For comparison, the dashed and dotted lines show the predicted DPRs for the best-fit star formation histories adopting the old ATON yields and the Z08 yields, respectively. Data points show the DPRs from C-AGB and O-AGB stars estimated by different studies and reported in Table 1: Matsuura et al. (2009, 2013, triangles), Srinivasan et al. (2009, squares), Boyer et al. (2012, stars), Riebel et al. (2012, circles).

sifications of the point sources observed in SAGE (SAGE-Spec, Kemper et al. 2010).

In principle, detailed radiative transfer modeling of each star should be carried out in order to accurately determine the rate of dust production around the star. In practice, this shows to be very computationally expensive when samples of thousands of stars have to be analysed, although first applications on population studies have been attempted (Riebel et al. 2012). In general, however, measurements of the global dust input from large stellar samples rely on photometric techniques based on IR colours (Matsuura et al. 2009) or on IR excesses (Srinivasan et al. 2009; Boyer et al. 2012).

A comparison between the dust production rates (DPR) inferred by different studies is made difficult by the use of different classification criteria, methods to infer the dust mass loss rate, and dust opacities. In most analyses, the following AGB stars sub-classes have been identified: carbon-rich (C-AGB) and oxygen-rich (O-AGB) AGB stars, *extreme* AGB stars (x-AGB), and anomalous O-rich (aO-AGB) sources (Cioni et al. 2006; Blum et al. 2006; Riebel et al. 2010; Boyer et al. 2011). The latter are a sub-class of O-AGB stars while the x-AGB class is dominated by carbon stars but likely includes a small number of O-rich sources. For the purpose of the present analysis, we have added together the aO-AGBs/O-AGBs and the C-AGBs/x-AGBs contributions and we show the corresponding dust production rate obtained by different analyses in Table 1.

The theoretical DPR by AGB stars in the LMC and SMC can be computed using the star formation histories for different metallicity bins described in section 3. To be consistent with the analysis of Harris & Zaritsky (2004,

2009), we adopt a Salpeter IMF in the stellar mass range $0.1M_{\odot} \leq m \leq 100M_{\odot}$.

For a given grid of dust yields, $m_{\text{dust}}(m, Z)$, we compute the time dependent total DPR as,

$$\dot{M}_{\text{dust}}(t) = \sum_i \int_{m(t, Z_i)}^{m_{\text{up}}} dm' \Phi(m') m_{\text{dust}}(m', Z_i) \quad (1)$$

$$\text{SFR}[t - \tau(m', Z_i), Z_i]$$

where the index i runs over the metallicity bins, $\tau(m, Z)$ is the mass and metallicity dependent stellar lifetime (Raiteri, Villata & Navarro 1996), $m_{\text{up}} = 100M_{\odot}$, and the lower mass limit is such that $\tau(m, Z_i) = t$. The contribution of AGB stars to the DPR, $\dot{M}_{\text{dust}}^{\text{AGB}}$, is obtained setting the upper and lower integration limits to $0.1M_{\odot} \leq m(t, Z_i) \leq 8M_{\odot}$. We do not explicitly follow the metal enrichment of the galaxy; instead, for each galaxy, we adopt the age metallicity relations implied by the metallicity dependent star formation histories.

The predicted time evolution of the AGB DPR in the Magellanic Clouds is shown in Fig. 4, where we have separated the contribution to carbon dust, silicates, SiC and iron grains production. The carbon dust and silicates production rates are compared with observational data of C-AGB and O-AGB stars (see Table 1). For a given set of AGB stars dust yields, the time evolution of the DPRs is very similar in the two galaxies, with present-day values for the best-fit star formation histories which differ by less than 30%.

The three sets of AGB stars dust yields shown in the figures predict a similar evolution of the carbon DPR, although with different amplitudes. Since AGB stars carbon dust yields do not depend significantly on the initial metallicity of the progenitor stars, the features observed in the

Table 1. Dust production rates by carbon and oxygen-rich AGB stars obtained in different analyses of the LMC and SMC data. Where appropriate, sources classified as aO-AGBs have been included in O-AGBs and sources classified as x-AGBs have been included in C-AGBs. Note that in the recent analysis of Matsuura et al. (2013), the dust production rates by O-AGBs is reported together with the contribution of Red SuperGiants (RSG), hence we have left these two contributions together in the corresponding lines.

Large Magellanic Cloud			
Sources	$\dot{M}_d[10^{-6}M_\odot/\text{yr}]$	Number of Sources	Reference
C-AGB	43 (up to 100)	1779	Matsuura et al. (2009)
O-AGB	>> 0.4 (expected 12)		
C-AGB	26	7200	Srinivasan et al. (2009)
O-AGB	1.4	8200	
C-AGB	9.49	6076	Boyer et al. (2012)
O-AGB	0.95	15243	
C-AGB	13.64 ± 0.62	8049	Riebel et al. (2012)
O-AGB	5.5 ± 0.2	19566	
C-AGB	40	906	Matsuura et al. (2013)
O-AGB+RSG	40	...	
Small Magellanic Cloud			
C-AGB	0.747	1872	Boyer et al. (2012)
O-AGB	0.078	3094	
C-AGB	4	399	Matsuura et al. (2013)
O-AGB+RSG	3	86	

DPRs reflect analogous features in the global star formation history, with a time delay whose amplitude depends on the lifetime of the most massive star producing carbon dust (about $7 M_\odot$ for Z08 AGB stars yields and $3 M_\odot$ for ATON models). Both galaxies experienced a phase of enrichment in the first 4 - 5 Gyr of evolution, then a quiescent epoch, followed by a second major episode of enrichment roughly 2-3 Gyr ago and an enhanced DPR in the last few hundreds Myr of the evolution.

Due to the increased mass loss rates in the C-star stage, the production rates of carbon grains predicted by the new ATON yields is one order of magnitude larger than those predicted by the old ATON yields, and the resulting evolution is much closer to the predictions by Zhukovska & Tielens (2013) based on the Z08 AGB stars yields (see the dotted lines). However, while observations of C-AGB stars in the LMC seem to favour such larger mass loss rates, the opposite is true for the SMC where carbon dust production rates predicted by the old ATON yields provides a better match to the observational data.

The production rates of silicates predicted by the ATON yields (note that the old and new yields are consistent within the uncertainties due to the star formation histories) are in good agreement with the observations of O-AGB stars both in the LMC and in the SMC. Similarly good agreement is found when Z08 AGB stars yields are adopted. However, in this case silicate dust production is effective only in the last 2 Gyrs of the evolution. Conversely, efficient HBB in ATON models allows silicate dust production since the earliest evolutionary times, as stars with $m_{\text{star}} > 3 M_\odot$ form silicate grains already at a metallicity $Z = 0.001$.

The production of iron grains follows a time evolution similar to that of silicate grains, as these two grain species

form under HBB conditions in ATON models, although with different rates. Conversely, the enrichment in SiC closely follows the evolution of carbon DPR, but with a smaller amplitude, reflecting the relative abundance of these two species in the dust yields produced by low-mass stars at any metallicity.

Note that with the adopted star formation histories, the carbon DPR in the last 4 Gyr of the evolution is dominated by $Z = 0.004$ AGB stars and that in both galaxies $Z = 0.008$ stars dominate only in the last few hundreds Myr of the DPR evolution. Given the small sensitivity of theoretical carbon dust yields to the metallicity of the progenitors, we do not expect a strong dependence on the adopted metal enrichment history for the galaxies.

We test this hypothesis by adopting a different metallicity evolution: we use the age metallicity relations inferred by Piatti & Geisler (2013) for the LMC and by Piatti (2012) for the SMC (see Fig. 3) as a proxy for the metal enrichment of the ISM of the galaxies; hence, we can recompute the DPRs implied by the total star formation histories of Harris & Zaritsky, without differentiating among the different metallicity-dependent components. As expected, Fig 5 shows that the carbon DPRs predicted by a given set of AGB stars dust yields do not differ significantly from the ones shown in Fig. 4.

Conversely, the lower metallicities implied by the age metallicity relations (particularly for the SMC, where there is no single stellar population with metallicity $Z > 0.004$) result in a significant depression of the silicate DPRs predicted by Z08 AGB stars yields, which are below the observational data for the SMC by several orders of magnitudes.

Hence, we conclude that current samples of AGB stars in the LMC favour strong mass loss rates from C-stars, as

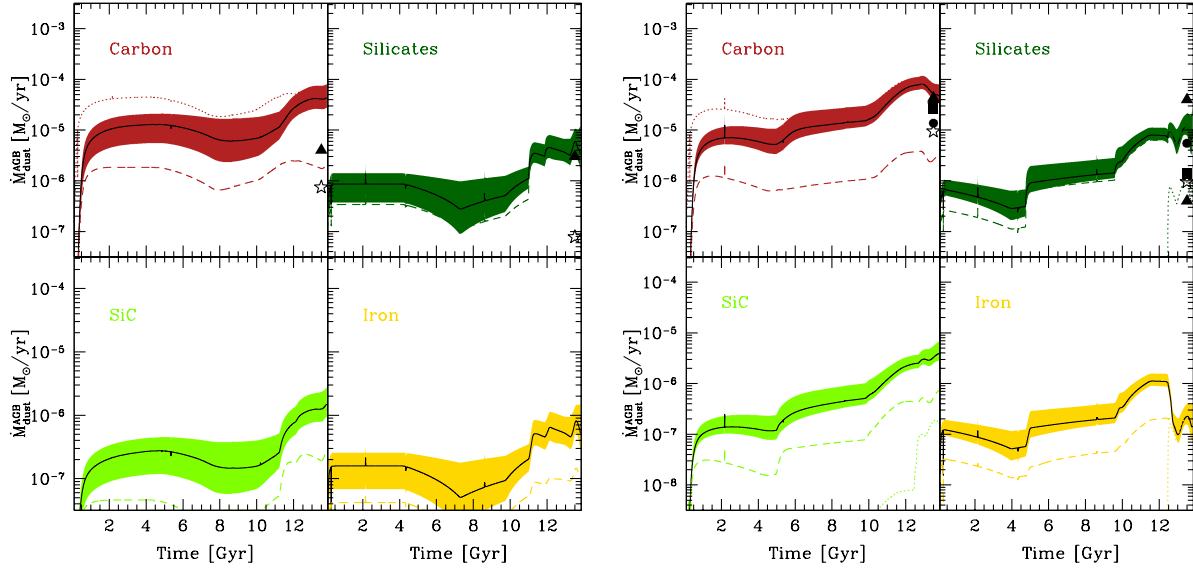


Figure 5. Same as in Fig.4 but adopting the Harris & Zaritsky (2004, 2009) global star formation histories and the Piatti (2012) and Piatti & Geisler (2013) age metallicity relations for the SMC and LMC, respectively, to estimate the metal enrichment history of the ISM. In the left panel, silicates, SiC and Iron DPRs for the Z08 AGB stars yields (dotted lines in Fig. 4) are much below the plotted range (see text).

predicted by the new ATON yields with the Wachter et al. (2008) mass loss rate prescription, and by the Z08 AGB stars yields. The same yields, however, exceed the DPRs observed for C-AGB stars in the SMC by approximately one order of magnitude. The latter data are better reproduced by the old ATON yields, which were based on the less efficient mass loss rate prescription by Blöcker et al. (1995).

This may be an indication of a metallicity dependence of the mass loss rates during the carbon-star phase of AGB evolution. We note that Blöcker et al. (1995) based their prescription on a description of the circumstellar envelope of MIRA variables that neglects the effects of radiation pressure on dust, probably underestimating mass loss rates in the carbon-stage phase. Conversely, the formulation by Wachter et al. (2008) is based on hydrodynamical wind models which include carbon-dust formation; however, there is no significant metallicity dependence in their formulation and the resulting mass-loss rates are of the same order of magnitudes for solar metallicity models, models with the metallicity of the LMC, and models with the SMC metallicity.

A unique feature of the ATON yields is that efficient HBB experienced by stars with $m > 3M_{\odot}$ lead to silicate dust production by AGB stars with initial metallicity $Z \geq 0.001$. Conversely, both Zhukovska et al. (2008) and Nanni et al. (2013) find that silicate grains can only form in AGB stars when their initial metallicities are higher; for the metallicity range relevant to the present analysis, silicate yields from Z08 AGB stars are not negligible only for stellar metallicity $Z = 0.008$. Hence, if the dominant stellar population in the SMC have metallicities $Z \leq 0.004$, as observed by Piatti & Geisler (2013), the observed population of O-AGB stars suggests that silicate dust formation should occur already at lower metallicities, as predicted by efficient HBB occurring in the ATON models.

Finally, since the total DPRs are dominated by carbon grains, their current values are not significantly affected by the metal enrichment history and depend more on the adopted dust yields. The total DPR by AGB stars in the LMC is predicted to be $[9.86, 51.3, 67.1] \times 10^{-6} M_{\odot}/\text{yr}$ for the ATON, new ATON, and the Z08 AGB stars dust yields. Although these values span the range indicated by observations of C-AGB and O-AGB stars, the new ATON and the Z08 yields lead to DPRs which are larger than most of the observational result (except for the most recent Matsuura et al. 2013 determinations, which however refer to the global contributions of C-AGB, O-AGB stars and RSGs). Similarly, the total DPR by AGB stars in the SMC is predicted to be $[7.62, 41.7, 48] \times 10^{-6} M_{\odot}/\text{yr}$ for the ATON, new ATON, and the Z08 AGB stars dust yields, with the latter two dust yields exceeding the observed DPRs by one order of magnitude.

How do these results depend on the uncertainties in the SMC star formation rate discussed in section 3? Even if we were to scale-down² the star formation rate predicted by Harris & Zaritsky (2009) by a factor 4, the present-day carbon DPR predicted by the new ATON AGB stars yields (and by Z08 AGB stars yields) would be $\approx 10^{-5} M_{\odot}/\text{yr}$, larger than the observational data on C-AGB stars by Boyer et al. (2012) and Matsuura et al. (2013). The old ATON yields would decrease the DPR to $5.43 \times 10^{-7} M_{\odot}/\text{yr}$, still in agreement with observations.

In the following, we will estimate the contribution of AGB stars to the total stellar dust budget if the MCs using

² The scale factor was chosen so as to reproduce the present-day global stellar mass in the SMC and - at the same time - have a recent star formation rate in agreement with H_{α} and $24\mu\text{m}$ observations (at least within the uncertainties).

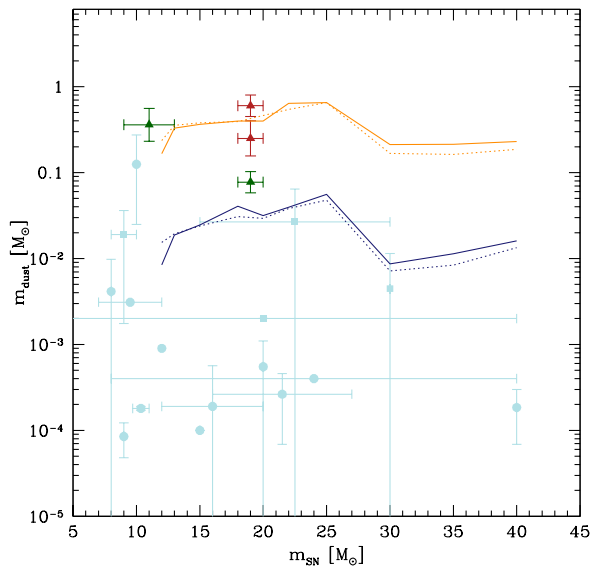


Figure 6. Mass of dust produced by supernovae as a function of the progenitor mass. The data points in light blue are taken from the compilation published in Gall, Hjorth & Andersen (2011) and Otsuka et al. (2012): circles refer to observations of SNe (12 objects) and squares to observations of SN remnants (4 objects). The triangles indicate Herschel detected sources in the Milky Way (dark green) and in the LMC (red, see text). The two sets of lines represent dust yields predicted by theoretical models for stars with initial metallicities $Z = Z_{\odot}$ (solid) and $Z = 0.1Z_{\odot}$ (dotted); the upper (lower) set of lines shows the mass of dust before (after) the passage of the reverse shock.

the new ATON and the old ATON models as the reference dust yields for the LMC and SMC, respectively.

5 TOTAL DUST BUDGET

The total mass of dust present in the interstellar medium of the LMC and SMC has been estimated using different techniques (extinction, emission, elemental depletions) and observational facilities (see Table 1 in Meixner et al. 2013 for a recent compilation). Total dust masses of $M_{\text{dust}} = 1.2 \times 10^6 M_{\odot}$ and $3 \times 10^5 M_{\odot}$ have been derived through analyses of *Spitzer* SAGE maps of the LMC and SMC, respectively (Bernard et al. 2008; Leroy et al. 2007). Recently, Skibba et al. (2012) have provided new estimates of the total dust mass using *Herschel* HERITAGE data; after convolving the photometric data for the two galaxies to a common resolution, the authors inferred a total dust mass of $M_{\text{dust}} = 1.1 \times 10^6 M_{\odot}$ for the LMC and $1.1 \times 10^5 M_{\odot}$ for the SMC, in good agreement with previous estimates. At the time of paper submission, a new analysis of the dust surface density maps of the MCs by the HERITAGE team was completed (Gordon et al. 2014) and the resulting integrated dust masses were $(7.4 \pm 1.7) \times 10^5 M_{\odot}$ and $(8.3 \pm 2.1) \times 10^4 M_{\odot}$ for the LMC and SMC, respectively. These values of the dust masses are significantly smaller than previous estimates, probably due to different assumptions in the models used to fit the maps.

In the following analysis, we will compare *Herschel* data

to the mass of dust produced by AGB stars and supernovae (SN) adopting the star formation and metal enrichment histories discussed in the previous sections. We take the new ATON (old ATON) yields to compute the mass of dust produced by AGB stars in the LMC (SMC) as these provide a good match to the observed AGB dust production rates.

Dust yields for massive stars have been theoretically calculated by different groups (Todini & Ferrara 2001; Nozawa et al. 2003; Bianchi & Schneider 2007; Cherchneff & Dwek 2010; Sarangi & Cherchneff 2012). The effective SN dust yields, i.e. the mass of dust that is able to survive the passage of the reverse shock enriching the ISM, can be significantly smaller than the dust mass newly formed in the expanding ejecta (Bianchi & Schneider 2007; Nozawa et al. 2007; Silvia et al. 2010). In Fig.6 we compare theoretical models with observational data. Dust masses of the same source obtained by different groups have been averaged and represented by a single data point. Herschel-detected sources are marked as triangles: Crab and CasA, (dark green, Gomez et al. 2012; Dunne et al. 2009; Barlow et al. 2010) and SN1987A and N49 (red, Matsuura et al. 2011; Otsuka et al. 2010). The latter data has to be viewed as an upper limit to the newly formed dust due to possible contamination from ISM dust. We consider Herschel-detected sources to provide a more complete census of the dust associated to the SN, being sensitive to the dynamically dominant cool dust component. Yet, none of the remnants is old enough (ages $< 10^3$ yr) for the reverse shock to have significantly affected the newly formed dust. Given this uncertainty, we will compute the mass of dust produced by massive stars adopting the Bianchi & Schneider (2007) dust yields for the no-reverse shock case shown with the upper lines and with a reverse shock model where the explosions take place in circumstellar medium with average density of $n_{\text{ISM}} = 1 \text{ cm}^{-3}$ (lower lines).

In what follows, our aim is to compare the maximum contribution to the existing dust mass by stellar sources. Hence, we simply integrate Eq. 1, without considering the effective dust lifetime in the ISM, due to the combined effects of destruction by interstellar shocks in the hot diffuse ISM or the process of grain growth by accretion of gas-phase elements in the dense ISM (see e.g. Valiante et al. 2011, 2014 for a complete chemical evolution model with dust). The integrated dust masses that we compute here are to be viewed as the maximum dust budget that stellar sources may potentially contribute.

The results for the LMC are shown in Fig.7. In the left panel, we plot the time evolution of the stellar mass³ predicted by the Harris & Zaritsky (2009) star formation rate. The observational data points are taken from Skibba et al. (2012), who used the calibration of Eskew et al. (2012) to convert from the 3.6 and 4.5 μm flux densities to stellar mass, finding $M_{\text{star}} = 2 \times 10^9 M_{\odot}$ with approximately 30% uncertainty. It is clear that the predicted stellar mass is consistent with the observational data point but only adopt-

³ The stellar mass shown in the figure is not simply the time integral of the star formation rate, but takes into account the fraction of stellar remnants predicted by the adopted Salpeter IMF. Hence, it can be viewed as the mass of active stars to be compared to the stellar mass inferred by the spectral energy distribution.

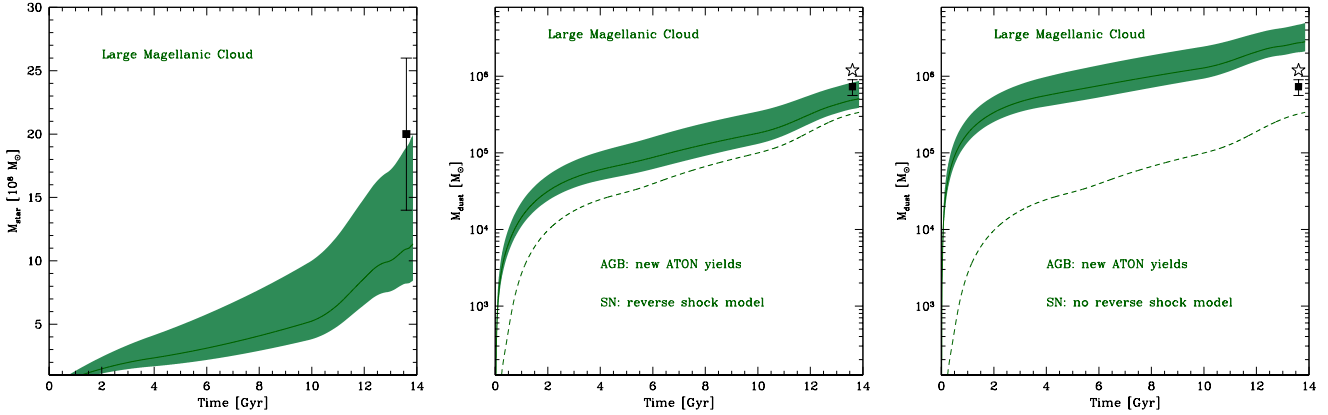


Figure 7. Time evolution of the stellar (left panel) and dust masses (central panel) predicted by the LMC model. We used the Harris & Zaritsky (2009) global star formation histories (solid lines indicate the predictions obtained adopting the best-fit SFH and the shaded regions illustrate the uncertainty on the fit) and the Piatti & Geisler (2013) age metallicity relation to estimate the metal enrichment history of the ISM. The observational data are taken from Skibba et al. (2012, star) and from Gordon et al. (2014, square). The right panel shows the dust mass evolution adopting the no reverse shock models for the dust yields of massive stars (see Fig.6). The dashed lines show the mass of dust produced by AGB stars only, adopting the best-fit SFH.

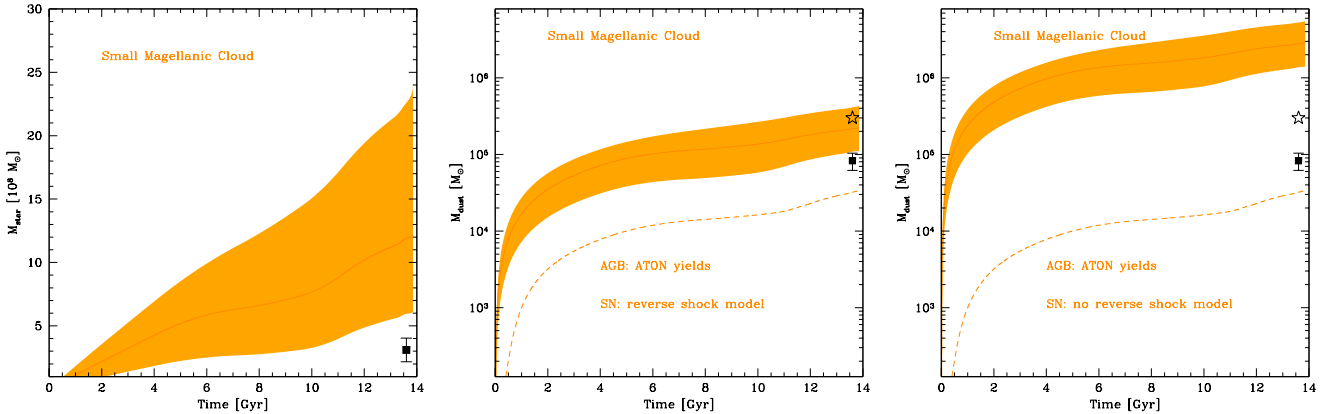


Figure 8. Same as Fig.7 but for the SMC model. We used the Harris & Zaritsky (2004) global star formation histories (solid lines indicate the predictions obtained adopting the best-fit SFH and the shaded regions illustrate the uncertainty on the fit) and the Piatti (2012) age metallicity relation to estimate the metal enrichment history of the ISM.

ing the upper limit on the SFH from the Harris & Zaritsky (2009) analysis.

The total mass of dust produced by stellar sources is too small to account for the present-day dust mass in the LMC derived by Skibba et al. (2012) but it is in good agreement with the more recent estimates by the HERITAGE team (Gordon et al. 2014), if no significant destruction in the ISM occurs. This is shown in the central panel of the same figure, where we compare the mass of dust predicted by the model adopting the new ATON yields for AGB stars and the reverse shock yields for SNe. The total mass of dust produced by stellar sources ranges between $3.9 \times 10^5 M_\odot$ and $8.7 \times 10^5 M_\odot$, with the best-fit value of $M_{\text{dust}} = 5.1 \times 10^5 M_\odot$. While the predicted dust masses are consistent with previous findings by Matsuura et al. (2009) and Zhukovska & Henning (2013), the previously reported large discrepancies between dust input from stars and the existing interstellar dust mass are no longer supported by the most recent data. In the conservative limit of reverse shock yields, mas-

sive stars do not represent the dominant dust sources, with AGB stars contributing to 67% of the final dust mass.

Similar conclusions apply for the SMC, although with larger uncertainties (see Fig. 8). In fact, the star formation history by Harris & Zaritsky (2004) predicts a stellar mass larger than the value inferred by Skibba et al. (2012), $M_{\text{star}} = 3.1 \times 10^8 M_\odot$. Although the latter value has been derived using a calibration based on a detailed analysis of the LMC (Eskew et al. 2012), the difference between the final stellar masses is larger than the observational uncertainty. With this caveat, stellar sources in the SMC model produce a total mass of dust in the range $1.1 \times 10^5 M_\odot \leq M_{\text{dust}} \leq 4.3 \times 10^5 M_\odot$, with a best-fit value of $M_{\text{dust}} = 2.3 \times 10^5 M_\odot$. This is in good agreement with the observed mass of dust in the SMC, with massive stars dominating the total dust budget at all times and AGB stars producing only 15% of the total ISM dust mass. Note that if we were to scale down the best-fit star formation rate of Harris & Zaritsky (2009) in order to reproduce the observed stellar

mass (see section 4), the total dust mass produced by stars would be in $2.8 \times 10^4 M_\odot \leq M_{\text{dust}} \leq 10^5 M_\odot$, with a best-fit value of $5.6 \times 10^4 M_\odot$. These values appear to be more consistent with the results by Boyer et al. (2012) and Matsuura et al. (2013), who estimate the lifetime of dust in the SMC using star formation rates in the range $[0.037 - 0.08 M_\odot/\text{yr}]$, lower than the results by Harris & Zaritsky (2009) and closer to the values reported by Bolatto et al. (2011) and Skibba et al. (2012). Yet, while previous studies concluded that the dust input from stars in the SMC was too low to account for the existing interstellar dust mass, we find that the most recent observations by the HERITAGE team (Gordon et al. 2014) support a stellar origin for dust in the SMC.

Finally, we have recomputed the dust mass evolution assuming that dust production in SN does not suffer any destruction by the reverse shock (no reverse shock models). The right panels of Figs. 8 and 7 show that the mass of dust produced by stars *exceeds* the observational data in both galaxies. It is important to stress that all the above findings have been obtained assuming that dust grains injected by stars in the ISM do not suffer further reprocessing, like destruction by interstellar shocks or grain growth in dense clouds. Hence, our analysis suggests that moderate destruction by the reverse shock of the SNe, or by interstellar shocks might have occurred during the evolution of the galaxies. A detailed investigation of dust reprocessing in the ISM requires the development of a full chemical evolution model with dust (Valiante et al. 2009, 2011, 2014), including a two-phase description of the dense and diffuse phases of the ISM (de Bressan et al. 2014), which goes beyond the scope of the present analysis.

6 CONCLUSIONS

In this paper, we have compared theoretical dust yields for AGB stars to observations of dust production rates by carbon-rich and oxygen-rich AGB stars in the Small and Large Magellanic Clouds. Our aim is to test whether current observations have the potential to discriminate among different models and to shed light on the complex dependence of the dust yields on the mass and metallicity of progenitor stars.

Using metallicity dependent star formation histories inferred by Harris & Zaritsky (2004, 2009) based on the MCPS survey, we find that:

- Observed dust production rates by carbon-rich AGB stars in the LMC favour theoretical models with strong mass loss, as predicted by the new ATON models with Wachter et al. (2008) mass loss prescription.
- The same yields, however, exceed the dust production rate observed for carbon-rich AGB stars in the SMC by approximately one order of magnitudes. Hence, current data of the SMC seem to favour the old ATON yields, which were based on the less efficient mass loss rate prescription by Blöcker et al. (1995). This conclusion is independent of the uncertainties associated to the star formation or the metal enrichment histories of the galaxy and may be an indication of a stronger metallicity dependence of the mass-loss rates during the carbon-star stage.
- Efficient Hot Bottom Burning in ATON models allows stars with $m_{\text{stars}} > 3 M_\odot$ to enrich the interstellar medium

with silicate and iron grains already at very low metallicities, $Z \geq 0.001$, at odds with dust yields based on synthetic AGB models. If the dominant stellar populations in the SMC have metallicities $Z \leq 0.004$, observations of dust production rates by oxygen-rich stars have the potential to confirm or refute the theoretical predictions.

- The latest analysis by the HERITAGE team (Gordon et al. 2014) leads to integrated dust masses in the LMC and SMC that are a factor 2-4 smaller than previous estimates. When compared to our model predictions, we find that the existing dust mass in the ISM of the MCs can have a stellar origin, even without resorting to extreme yields, unless significant destruction of the newly formed dust in SN reverse shock or in the ISM takes place.

Our study confirms the potential of the Magellanic Clouds as fundamental astrophysical laboratories to test our current understanding of the dust cycle in the interstellar medium. Yet, conclusions based on detailed comparison between models and observations are hampered by uncertainties on the star formation and chemical enrichment history of the galaxies, particularly of the Small Magellanic Cloud. Future observational studies complemented by a more realistic modelling of the two brightest satellites of the Milky Way in a cosmological context (Boylan-Kolchin et al. 2011) are needed to make substantial progress.

ACKNOWLEDGMENTS

We thank Alberto Bolatto, Michele Cignoni and Mikako Matsuura for their kind collaboration and for useful discussions. The research leading to these results has received funding from the European Research Council under the European Union's Seventh Framework Programme (FP/2007-2013) / ERC Grant Agreement n. 306476. HH thanks support from the NSC grant NSC102-2119-M-001-006-MY3. FK acknowledges financial support from the NSC under grant number NSC100-2112-M-001-023-MY3.

REFERENCES

- Barlow M. J. 2010, *A&A*, 518, L138
- Bernard J.-P., Reach W. T., Paradis D., et al. 2008, *AJ*, 136, 919
- Boylan-Kolchin M., Besla G., Henrquist L. 2011, *MNRAS*, 414, 1560
- Bianchi, S. & Schneider, R. 2007, *MNRAS*, 378, 973
- Blöcker T., 1995, *A&A*, 297, 727
- Blöcker T., Schönberner D., 1991, *A&A*, 244, L43
- Blum R. D., Mould J. R., Olsen, K. A. et al. 2006, *AJ*, 132, 2034
- Bolatto A. et al. 2011, *ApJ*, 741, 12
- Boyer M. L., Srinivasan S., van Loon J. T. et al. 2011, *AJ*, 142, 103
- Boyer, M. et al. 2012, *ApJ*, 748, 40
- Carrera R., Gallart C., Hardy E., Aparicio A., and Zinn R. 2008a, *AJ*, 135, 836
- Carrera R., Gallart C., Aparicio A., Costa E., Méndez R. A., and Noël N. D. E. 2008b, *AJ*, 136, 1039
- Cherchneff I. & Dwek E. 2010, *ApJ*, 713, 1
- Cioni M.-R. L., Girardi L., Marigo P. & Habing H. J. 2006, *A&A*, 448, 77
- De Bressan M., Schneider R., Valiante R., Salvadori S. 2014, in prep.

- Di Criscienzo M., Dell'Agli F., Ventura P., Schneider R., Valiante R., La Franca F., Rossi C., Gallerani S., Maiolino R. 2013, *MNRAS*, 433, 313
- Dunne L. et al. 2009, *MNRAS*, 394, 1307
- Eskew M., Zaritsky D. & Meidt S. 2012, *AJ*, 143, 139
- Ferrarotti A.D., Gail H.P., 2001, *A&A*, 371, 133
- Ferrarotti A.D., Gail H.P., 2002, *A&A*, 382, 256
- Ferrarotti A.D., Gail H.P., 2006, *A&A*, 553, 576
- Gall C., Hjorth J., Andersen A. C. 2011, *A&ARv*, 19, 43
- Galliano F. et al. 2011, *A&A*, 536, A88
- Gomez H. et al. 2012, *ApJ*, 760, 96
- Gordon K. D. et al. 2011, *AJ*, 142, 102
- Gordon K. D. et al. 2014, *ApJ*, submitted
- Harris J. & Zaritsky D. 2001, *ApJSS*, 136, 25
- Harris J. & Zaritsky D. 2004, *ApJ*, 127, 1531
- Harris J. & Zaritsky D. 2009, *ApJ*, 138, 1243
- Kemper, F., Woods, P. M., Antoniou, V., et al. 2010, *PASP*, 122, 683
- Leroy A. et al. 2007, *ApJ*, 658, 1027
- Marigo P., Girardi L. 2007, *A&A*, 469, 239
- Marigo P., Bressan A., Nanni A., Girardi L., Pumo M. L. 2013, *MNRAS*, 434, 488
- Matsuura M. et al. 2009, *MNRAS*, 396, 918
- Matsuura M., Woods P.M., Owen P.J. 2013, *MNRAS*, 429, 2527
- Meixner M. et al. 2006, *AJ*, 132, 2268
- Meixner M. et al. 2010, *A&A*, 518, L71
- Meixner M. et al. 2013, *ApJ*, 146, 62
- Nanni A., Bressan A., Marigo P., Girardi L., 2013, *MNRAS*, 434, 2390
- Nozawa T., Kozasa T., Umeda H., Maeda K. & Nomoto K. 2003, *ApJ*, 598, 785
- Nozawa T., Kozasa T., Habe A., et al. 2007, *ApJ*, 666, 955
- Otsuka M. et al. 2010, *A&A*, 518, L139
- Otsuka M. et al. 2012, *ApJ*, 744, 26
- Piatti A. E. 2012, *MNRAS*, 422, 1109
- Piatti A. E. & Geisler G. 2013, *AJ*, 145, 17
- Raiteri C.M., Villata M., Navarro J.F. 1996, *A&A*, 315, 105
- Riebel D., Meixner M., Fraser O., et al. 2010, *ApJ*, 723, 1195
- Riebel D., Srinivasan S., Sargent B., and Meixner M. 2012, *ApJ*, 753, 71
- Silvia D. W., Smith B. D., & Shull J. M. 2010, *ApJ*, 715, 1575
- Skibba R. A. et al. 2012, *ApJ*, 761, 42
- Srinivasan, S. et al. 2009, *ApJ*, 137, 4810
- Skrutskie, M. F. et al. 2006, *AJ*, 131, 1163
- Todini, P. & Ferrara, A. 2001, *MNRAS*, 325, 726
- Valiante R., Schneider R., Bianchi S., Andersen A., Anja C., 2009, *MNRAS*, 397, 1661
- Valiante R., Schneider R., Salvadori S., Bianchi S., 2011, *MNRAS*, 416, 1916
- Valiante R., Schneider R., Salvadori S., Gallerani S., 2014, submitted
- Ventura P., Zeppieri A., Mazzitelli I., D'Antona F., 1998, *A&A*, 334, 953
- Ventura P., D'Antona F., 2009, *A&A*, 499, 835
- Ventura P., Di Criscienzo M., Schneider R., Carini R., Valiante R., D'Antona F., Gallerani S., Maiolino R., Tornambé A., 2012, *MNRAS*, 420, 1442
- Ventura P., Di Criscienzo M., Schneider R., Carini R., Valiante R., D'Antona F., Gallerani S., Maiolino R., Tornambé A., 2012, *MNRAS*, 424, 2345
- Ventura P., Dell'Agli F., Schneider R., Di Criscienzo M., Rossi C., La Franca F., Gallerani S., Valiante R. 2014, *MNRAS*, in press
- Wachter A., Winters J. M., Schroeder K. P., Sedlmayr E., 2008, *A&A*, 497, 504
- Weisz D.R., Dolphin A. E., Skillman E. D., Holtzman J., Dalcanton J. J., Cole A. A. and Neary K., 2013, *MNRAS*, 431, 364
- Zaritsky D., Harris J., Thompson I. B., & Grebel E. K. 2004, *AJ*, 128, 1606
- Zhukovska S., Gail H. P., Tieloff M., 2008, *A&A*, 479, 453
- Zhukovska S. & Henning T., 2013 *A&A*, 555, 99